Author's post-print version. This manuscript has been published by the Journal of Analytical and Applied Pyrolysis (https://doi.org/10.1016/j.jaap.2017.01.003).
The published version of this paper is available at:
https://www.sciencedirect.com/science/article/pii/S016523701630599X

STOCHASTIC REACTOR MODELING OF BIOMASS PYROLYSIS AND GASIFICATION

K. Weber[a]*, T. Li[a], T. Løvås[a], C. Perlman[b], L. Seidel[c], F. Mauss[c]

*corresponding author: kathrin.weber@ntnu.no

[a] Department of Energy and Process Engineering, Norwegian University of Science and Technology, Kolbjørn Hejes vei 1a, Trondheim, Norway.

[b] LOGE AB, Lund Combustion Engineering, Scheelevägen 17, Lund, Sweden.

[c] Thermodynamics and Thermal Process Engineering, Brandenburg University of Technology, Siemens-Halske-Ring 8, Cottbus, Germany

Abstract: In this paper, a partially stirred stochastic reactor model is presented as an alternative for the modeling of biomass pyrolysis and gasification. Instead of solving transport equations in all spatial dimensions as in CFD simulations, the description of state variables and mixing processes is based on a probability density function, making this approach computationally efficient. The virtual stochastic particles, an ensemble of flow elements consisting of porous solid biomass particles and surrounding gas, mimic the turbulent exchange of heat and mass in practical systems without the computationally expensive resolution of spatial dimensions. Each stochastic particle includes solid phase, pore gas and bulk gas interaction. The reactor model is coupled with a chemical mechanism for both surface and gas phase reactions. A Monte Carlo algorithm with operator splitting is employed to obtain the numerical solution. Modeling an entrained flow gasification reactor demonstrates the applicability of the model for biomass fast pyrolysis and gasification. The results are compared with published experiments and detailed CFD simulations. The stochastic reactor model is able to predict all major species in the product gas composition very well for only a fraction of the computational time as needed for comprehensive CFD.

Keywords: Biomass, Pyrolysis, Gasification, Modeling, Stochastic Reactor

1 Introduction

Biomass gains increasing attention as a renewable alternative to fossil fuels, as it enables a sustainable and efficiently implementable pathway for heat and power generation as well as secondary biofuel production. Direct combustion of biomass is a common option for production of heat and power. However, integrated biorefinery concepts leading to multiple products is the anticipated key solution for an economically viable future bio-economy [1]. Biochar (or biocarbon), the carbonaceous solid product from biomass pyrolysis (and gasification)may for example replace fossil carbon carriers in a number of industrial applications such as in metallurgical processes. The gaseous and liquid products may serve as a feedstock for the production of liquid fuels and chemicals.

The first steps in pyrolysis and gasification are drying and devolatilization. Water vapor is first released, followed by permanent gases (such as CO, CO_2, H_2 and CH_4) and condensable gases (tars) while carbonaceous solid (char) remains. These primary products of pyrolysis may undergo further conversion if the residence time is sufficiently long. Tars may polymerize and crack, decreasing the amount of functional groups and thereby forming secondary (and tertiary) tars of higher aromaticity, while releasing more gas (and solid). In addition, the gaseous and solid products may undergo further conversion reactions. Even though pyrolysis has been used since ancient times for the production of charcoal, the details of the elementary chemical processes, reactions, intermediates and products are very complex and remain largely unknown. For example, a common understanding of even the first kinetic step (devolatilization) is yet not established. Kinetic parameters differ largely and are under constant evaluation, and the proposed models are typically only valid for restricted conditions [2]–[8].

Much effort has been devoted both experimentally and theoretically to reveal these details allowing optimization of pyrolysis processes for modern industrial purposes. Product yield distribution, feedstock variability, control of temperatures, heating rates and material flows are among the critical issues important for the efficiency of these processes [9], [10]. A common approach to understand the challenges involved is model development to simulate processes in detail. Modeling of thermochemical biomass conversion should however strictly speaking involve the coupling of both the complex chemical kinetics as well as that of turbulent transport of energy, mass and momentum, which occur during the process in a multi-phase environment. Modeling efforts began in the 1940s [11] and have since produced ever more complex descriptions of both physical and chemical phenomena.

For a realistic description of practical systems, in which the characteristic time scales of mixing can be of the same order of magnitude as the time scales of chemical kinetics, both the rate limiting effects of chemical kinetics and physical mixing have to be taken into account. This is the subject for large detailed studies employing Eulerian or Eulerian-Lagrangian type simulations published in literature recently where dynamics, gaseous kinetics and solid particle reactions are included, revealing many details of the multi-phase flows for different biomass conversion systems (e.g. [12]–[15]). Ranzi et al. ([16], [17]) have also presented comprehensive models that account for physical processes and detailed chemical kinetics on both the fuel particle and the reactor level. Such multi-scale numerical simulations require however significant computing time. Hence, simplifying assumptions are often necessary. Descriptions of different levels of modeling approaches for biomass pyrolysis can be found elsewhere, e.g. in [7], [18] or [19]. A review of models for biomass gasification is given e.g. in [20]. The reader is referred to these sources for further details on general modelling approaches. Here we will focus on models based on the stirred reactor approach, which has been widely used in the combustion community to simulate stationary systems, however not as well established for gasification and pyrolysis of solid fuels.

In perfectly mixed conditions, the rate of the thermochemical conversion is only controlled by chemical kinetics, while the mixing process can be regarded as infinitely fast and its influence therefore be neglected. These assumptions lead to the well-stirred or perfectly stirred reactor model (PSR). The focus is therefore on kinetic modeling, often

limited to the gas phase kinetics of biomass conversion [21], [22]. A more detailed treatment of biomass pyrolysis is proposed by Lee et al. [23]. They combine a thermodynamic model for biomass conversion with a PSR model for the gaseous products. Septien et al. [24] modeled biomass gasification using a single fuel particle representation, hence without fuel particle interactions, but coupled with a detailed chemical mechanism for both heterogeneous and homogenous reactions. Similar approaches are also available in commercial tools including solid and fluid interaction (e.g. [25]), however turbulent mixing effects are usually neglected [20].

An equally idealizing approach is the assumption of fast chemical kinetics, resulting in a process that is mostly controlled by mixing of the reactants [26]. This is enabled by partial stirring in the simplified reactor, i.e. accounting for inhomogeneities e.g. through a joint composition probability density function (PDF). In earlier works a stirred reactor was presented by Spielman and Levenspiel including mixing, reactions and through-flow, based on a Monte Carlo simulation of a coalescing system [27]. In combustion research these models have received increased attention to efficiently tackle turbulent mixing effects which have been shown to be important for many aspects of the efficient conversion of the fuel such as kinetic rates, soot formation, extinction phenomena and emission control (e.g. [28]). These models are bound by two idealizing limiting regimes; the aforementioned perfectly stirred reactor (PSR) with infinitely fast mixing in both axial and radial directions, and the (tubular) plug flow reactor (PFR) with perfect mixing in radial direction, but where the reactants do not mix along the flow axis. Imperfectly mixed conditions are accounted for in partially stirred reactor models (PaSR) with mixing effects in all directions, and the partially stirred plug flow reactor (PaSPFR) with finite radial mixing [29], [30].

In this work, we demonstrate that simplifying complex turbulent mixing and thermal conversion processes in a partially stirred stochastic reactor allows detailed modeling of the multi-phase nature of biomass conversion. State variables are thereby not determined by solving the three dimensional Navier-Stokes equations as in computational fluid dynamics (CFD) simulations, but based on probability density functions (PDF) of the physical quantities. Only a one-dimensional flow, as in PFR is considered. The PDFs describe the probability of a certain variable to have a given value in time, as for example in a bell-shaped Gaussian distribution. The spatial information is lost, but replaced by a reactor model, which assumes exchange of heat and mass between an ensemble of virtual, so-called stochastic particles, resembling a mixing process. The strength of the stochastic reactor approach is its inclusion of turbulent mixing effects at low computational cost compared to CFD, which can be of the order hours versus days. This allows to couple a relatively detailed chemical mechanism with a complete reactor setup while maintaining feasible computational time. Such stochastic reactor models have been used to describe turbulent homogeneous combustion with great success (e.g. [30]–[33]), but have yet not been explored for their applicability to model heterogenouos conversion of solid fuels such as pyrolysis and gasification of biomass where a multi-phase treatment of the flow has to be taken into account.

The aim of the present work is to extend a novel stochastic reactor approach, which allows for reactions between gas and solid phases to account for all necessary steps of biomass conversion. It thereby offers a tool to describe heat and mass transfer within and between different phases, the mixing of reactants in the reactor, and the chemical kinetics

of drying, devolatilization, char conversion and gas phase reactions. To evaluate the accuracy of the stochastic reactor approach, pyrolysis and gasification experiments from literature have been modelled to determine the product gas composition under varying conditions [34]. The results of the simulation are compared with the experimental measurements as well as with the results from a more comprehensive CFD simulation of the same experiment previously published in literature [35].

The paper is organized as follows: The stochastic reactor model is described in detail in section 2.1, section 2.2 describes the kinetic model, which has been coupled with the reactor model. Section 2.3. gives a brief description of the experimental setup that has been used to validate the model for biomass conversion. In section 3.1, the model predictions are compared against the product gas composition of biomass pyrolysis and gasification. Section 3.2 shows some features of the stochastic modeling approach. Finally, concluding remarks are presented in section 4.

2 Material and Methods

2.1 Computational Modeling

In this study, the LOGEsoft gasification module [36] is extended to include all steps of thermal conversion of solid fuels in a simplified tubular reactor. In this zero dimensional stochastic reactor model, the state variables which are heterogeneously distributed in the reactor are described and modelled with probability density functions. The model is made suitable for biomass pyrolysis and/or gasification through proper treatment of the gas-solid phase interaction for biomass conversion through drying, devolatilization, char reactions and gas phase reactions.

The software introduces both a network of partially stirred reactor (PaSR network) as well as a partially stirred plug flow reactor (PaSPFR). For the network, the reactor is divided into a number of cells (also referred to as compartments), each of which is a partially stirred reactor (Figure 1 left). Each cell is filled with a certain amount of virtual stochastic particles, an ensemble of numerical particles composed of a given composition of solid phase, bulk and pore gas, with a distribution of states according to a specified distribution profile. The stochastic particles themselves are each considered homogeneous, but mix stochastically with each other and exchange heat and mass within the cell. The more inhomogeneous a mixture is, the more stochastic particles are required for an accurate description of the system. In- and outflow of solid and gaseous species are also considered between the cells as Figure 1 indicates, hence in this approach finite mixing is accounted for in both radial and axial direction.

For the PaSPFR, only a plug (or disk cell) is considered as it is transported along the length of the reactor (Figure 1 right). This plug is a partially stirred reactor with an initial biomass-to-gas ratio, meaning no additional in-and outflow is considered, only evolution of the plug in time. Since there is no in- and outflow this approach accounts for finite mixing only in radial direction. As for the PaSR, the plug (cell) is discretized into a number of stochastic particles, each with a specific composition of solid phase, bulk and pore gas distributed based on a PDF. Transport equations

are solved for each stochastic particle. For the present case, the PaSPFR setup was chosen, as it gives a more accurate representation of the setup of the experimental drop tube reactor used for validation where constant bulk flow in one direction is dominant with little turbulent mixing in axial direction. This will be outlined in more detail in section 2.3.

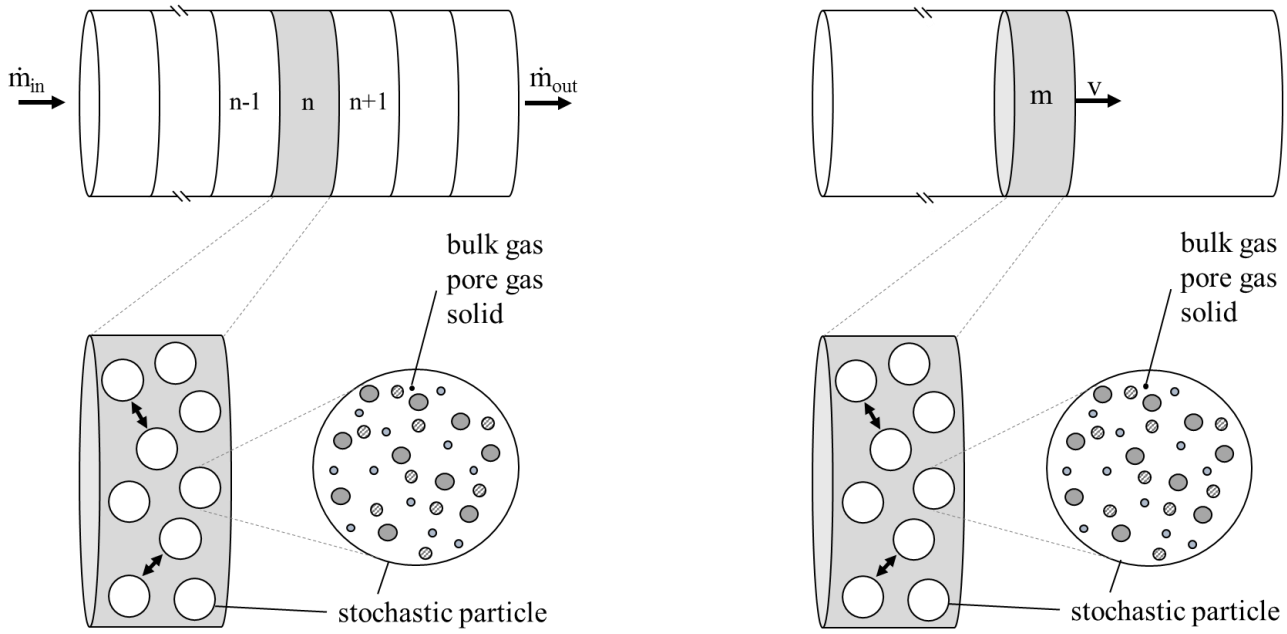

Figure 1 Series of partially stirred reactors (left) and partially stirred plug flow reactor (right)

Stochastic model and turbulent mixing

The stochastic reactor model is based on the description of local quantities of chemical species mass fractions and temperature as random variables, $\phi_{1,\dots}\ \phi_{S+1}$, with their sample space realization $\psi_{1,\dots}\ \psi_{S+1}$, where S is number of chemical species in the reaction mechanism. The adopted formulation of the time evolution of their joint scalar mass density function (MDF) F_ϕ is expressed as [36], [37]:

$$\frac{d}{dt}F_\phi(\psi,t)+\frac{d}{d\psi_i}((Q_i(\psi)F)_\phi(\psi,\mathrm{t}))+\frac{1}{\tau}(F_{in}-F_\phi(\psi,t))=mixing\ \ term \tag{1}$$

The equation describes the rate of change of both solid and gas species mass and energy (first term on the left hand side) due to chemical reactions and heat transfer interaction with the wall (second term) and cell in- and outflow (third term). Q_i represents the source terms for variable i (both species and temperature) and will be discussed in

more detail in the next section. The third term on the left hand side of the equation, which accounts for cell in- and outflow, is disregarded when modeling the reactor as a PaSPFR as discussed in the previous section.

The mixing term (right hand side (RHS) in equation (1)) accounts for the turbulent mixing in the reactor. The coalescence/dispersal model (C/D model) [36], [38] is used, where out of the total number of stochastic particles, particle pairs mix randomly to their mean value according to:

$$mixing\ term = \frac{C_\Phi \beta_m}{\tau_{mix}} \left(\int_{\Delta\Phi} F_\Phi(\psi - \Delta\psi, t)\, \mathrm{F}_\Phi(\psi + \Delta\psi) d(\Delta\psi) - F_\Phi(\psi, t) \right) \quad (2)$$

where C_ϕ and β_m are model constants in accordance to [36], [38] and τ_{mix} is the mixing time and considered a user defined parameter. C_ϕ is a proportionality constant and C_ϕ/τ becomes a measure of the scalar mixing intensity. A slow mixing process is described by a long mixing time, making the overall mixing term small. For equation (1), this implies that the mixing process contributes little to the value of the MDF. Consequently, a fast mixing process has a large influence on the value of the process variables, achieving almost homogeneous conditions in the reactor.

The effect of heterogeneity of the stochastic reactor approach becomes more apparent the more stochastic particles are used. This does not only affect the mixing process (equation 2), but also the heat transfer distribution over the stochastic particles. Overall, a Nusselt-number approach is applied to calculate the total heat transfer, which is then randomly distributed over the stochastic particles. A model parameter C_h is used to describe the fluctuation intensity of heat transfer between a stochastic particle and the reactor wall:

$$h_n = \frac{T_n - T_w^i}{C_h} \quad (3)$$

C_h influences the residence time of stochastic particles in the wall boundary layer. Long residence times (small C_h) result in high heat transfer. For $C_h=1$ each particle is cooled to the wall temperature, which is the maximum possible heat transfer. High values for C_h result in an equal distribution of the total heat flux over all stochastic particles.

In order to obtain a solution for equation (1) a Monte Carlo method with an operator splitting technique is employed. The stochastic reactor approach including a description of the numerical algorithm has been presented in earlier works by co-authors and further details can be found in [37].

Biomass conversion

As the biomass is converted, its mass m_s changes according to the reaction rate $\omega_{j,s}$ of the solid phase reactions:

$$\frac{dm_s}{dt} = -A_{s,total} \sum_{i=1}^{n} \omega_{\mathrm{j},s} \quad (4)$$

As a result, the initial particle diameter d_s decreases as the conversion progresses:

$$\frac{dd_s}{dt} = \left(\frac{6}{\pi \rho_s n_s}\right)^{\frac{1}{3}} \frac{m_s^{-\frac{2}{3}}}{3} \frac{dm_s}{dt} \tag{5}$$

The solid matter is assigned an initial porosity ε, which is also subject to change over time:

$$\frac{d\varepsilon}{dt} = -\frac{A_{s,total}}{V_{s,total}} \frac{(1-\beta)}{\rho_S} \sum_{i=1}^{n_s} \omega_{j,s} \tag{6}$$

The pores are filled with pore gas m_p from solid fuel surface reactions, the mass of which depends on the conversion rate of the solid and the exchange between pore and surrounding bulk gas (driven by a difference in concentration c_i and controlled by a mass transfer coefficient k_m) as represented by the first and second terms in the following equation:

$$\frac{dm_p}{dt} = A_{s,total} \sum_{i=1}^{n_g} \omega_{j,s} + A_{s,total} \sum_{j=1}^{n_g} W_j k_{m,j} (c_{j,g} - c_{j,p}) \tag{7}$$

Devolatilized gases from the solid are first released into the pores. The mass of the bulk gas thus depends only on the exchange with the pore gas:

$$\frac{dm_g}{dt} = -A_{s,total} \sum_{j=1}^{n_g} W_j k_{m,j} (c_{j,g} - c_{j,p}) \tag{8}$$

The chemical composition is calculated for each stochastic particle in the cell (the disk, in the case of the PaSPFR) and each time step. The temporal change in species mass fractions of the solid phase $Y_{i,s}$ is expressed as:

$$\frac{dY_{i,s}}{dt} = \frac{1}{\rho_s} \omega_{i,s} \frac{A_{s,total}}{V_{s,total}(1-\varepsilon)} - \frac{Y_{i,s}}{\rho_s} \frac{A_{s,total}}{V_{s,total}} \sum_{j=1}^{n_s} \omega_{j,s} \frac{1}{1-\varepsilon} \tag{9}$$

The first term on the RHS of equation (9) is the consumption of the solid species due to devolatilization, drying or chemical reaction. The second term ensures mass conservation as the consumption of solid results in a change of mass fraction.

The rate of change of pore gas species mass fractions is described as:

$$\frac{dY_{i,p}}{dt} = \frac{1}{\rho_p}\omega_{i,p} + \frac{A_{s,total}}{\rho_S V_{s,total}(1-\varepsilon)}(\omega_{i,s} - Y_{i,p}\sum_{j=1}^{n_g}\omega_{j,s} + W_i k_{m,i}(c_{i,g} - c_{i,p}) - Y_{i,p}\sum_{j=1}^{n_g} W_j k_{m,j}(c_{j,g} - c_{\mathrm{j,p}})) \quad (10)$$

The change depends on the gas phase reactions in the pores (first term on the RHS), the reaction rate in the solid phase (releasing gases into the pores, second and third term on the RHS), and the mass exchange between the pore and the bulk gas (fourth and fifth term on the RHS).

Finally, the bulk gas species mass fractions depend on the reaction rate in the gas phase as well as the mass exchange with the pore gas:

$$\frac{dY_{i,g}}{dt} = \frac{1}{\rho_g}\omega_{i,g} + \frac{A_{s,total}}{m_g} W_i k_{m,i}(c_{i,p} - c_{i,g}) + Y_i \frac{A_{s,total}}{m_g}\sum_{j=1}^{n_g} W_j k_{m,j}(c_{j,g} - c_{\mathrm{j,p}}) \quad (11)$$

Regarding the temperature evolution of the bulk gas phase, this is calculated as:

$$\frac{dT_g}{dt} = \frac{-1}{C_p \rho_g}\sum_{i=1}^{n_g} h_i \omega_i + \frac{A_{s,total}}{C_p m_g}(\sum_{j=1}^{n_g} W_j k_{m,j} c_{j,p}(h_{j,p} - h_g) + \alpha(T_s - T_g)) \quad (12)$$

where the contributions are from the heat of reaction of gas phase reactions (first term on the RHS), the heat transfer due to mass exchange with the pore gas (second term) and the heat transfer between the solid and the gas (third term), respectively. The heat transfer to the wall is treated with a stochastic jump process as part of the operator splitting method, which was explained in the previous chapter.

The solid phase and the pore gas are assumed to have the same temperature. This temperature is considered uniform, so temperature gradients within a particle are disregarded:

$$\begin{aligned}\frac{dT_{s,p}}{dt} = &-\frac{1}{C_{p,s}\rho_s}\sum_{i=1}^{n_g} h_{i,p}\omega_{i,p} + \frac{\Delta H_{pyr}}{C_{p,s}\rho_s}(\frac{1}{V_{s,total}}\frac{dm_s}{dt} - \frac{m_s}{{V_{s,total}}^2} n_s \frac{\pi}{6} 3d^2 \frac{dd}{dt}) \\ &+ \frac{A_{s,total}}{C_{p,s}V_{s,total}\rho_s}(\sum_{j=1}^{n_g} W_j k_{m,j} c_{j,g}(h_{j,g} - h_{j,p}) - \alpha(T_s - T_g) - q_{rad})\end{aligned} \quad (13)$$

The influences on the temperature are from the gas phase reactions in the pores (first term on the RHS), the heat released/consumed from the pyrolyzing solid (second and third term), the heat transfer due to mass diffusion between pore and bulk phase (fourth term), the heat transfer between the solid and the gas and radiant heat transfer between the reactor wall and the biomass, which is influenced by the properties (temperature T and emissivity ε) of both:

$$q_{rad} = \sigma\varepsilon_s\varepsilon_w(\mathrm{T_s}^4 - T_w^4) \quad (14)$$

2.2 Chemical Kinetics

In the current set-up a relatively simple chemical mechanism was coupled with the stochastic reactor model. The chemical mechanism corresponds to the one used in a CFD simulation by Ku et al. [35] on the same experiment as used here for validation purposes. This way, the performance of the simple stochastic reactor model can be directly compared to the performance and predictability of the complex CFD simulation. However, it is important to note that these choices are user defined and more detailed and rigorous mechanisms will be implemented for future applications and kinetic studies. In [35] the wood is described as a lumped species, which decomposes in a one-step reaction into gases and char during pyrolysis. Both the produced gases and char may subsequently undergo secondary gas phase and surface reactions. Tar formation is disregarded due to the relatively high temperature. The drying process is modelled in a separate reaction as the initial water is considered an independent species from the biomass. Ash is considered as an inert species, as oxidation and catalytic effects are neglected.

Drying

Biomass may contain a significant amount of water, the drying of which takes place as an initial step during pyrolysis and therefore can influence the conversion process. The drying process is treated as a heterogeneous reaction, the rate of which is determined by an Arrhenius-type law:

$$\omega_{H_2O} = A \cdot e^{\frac{-E_a}{RT}} \cdot c_{H_2O} \cdot W_{H_2O} \qquad \text{(R1)}$$

This is a common way to describe the drying process with a number of kinetic parameters available in the literature. In the present case, a frequency factor of $A=5.13 \times 10^6$ s^{-1} and an activation energy of E=87.9 kJ/mol (suggested by [39]) were used.

Devolatilization

In the validating experiment, beech wood sawdust particles with a representative diameter of 310 μm were used as will be described in more detail in section 2.3. Based on the fuel composition shown in Table 1, a generic sum formula of the wood composition can be written as $C_{42}H_{64}O_{28}$. It is assumed that the biomass devolatilizes into the main gas components CO, CO_2, H_2 and CH_4, which are the main components measured in the experiments. Further details will therefore be not validated. The relative distribution between these components, given in Table 2, was assumed in [35] based on the elementary composition considerations, and adopted for this work in order to enable the direct comparison between the statistical approach proposed and the numerical modeling approach presented in [35].

Table 1 Beech wood composition (as received basis) [34]

Moisture	9.04 wt%
Ash	0.61 wt%
Volatile matter	76.70 wt%
C	45.05 wt%
H	5.76 wt%

O	39.41 wt%

Table 2 Volatile matter composition [35]

CO	37.5 wt%
CO_2	41.1 wt%
H_2	2.9 wt%
CH_4	18.2 wt%

The resulting devolatilization reaction is formulated as:

$$C_{42}H_{64}O_{28} \rightarrow 11.6\ CO + 8.2\ CO_2 + 12.46\ H_2 + 9.77\ CH_4 + 12.43\ C(s) \quad \text{(R2)}$$

Gas phase reactions

Secondary reactions in the pore and bulk gas are described using five global reactions, shown in Table 3. References to the kinetic parameters for each reaction can be found in [35].

Table 3 Secondary gas phase reactions [35]

$CH_4 + 2\ O_2 \rightarrow CO_2 + 2\ H_2O$	$k = 5.16 \cdot 10^{13} \frac{K \cdot m^3}{kmol \cdot s} T^{-1} [CH_4][O_2] \exp(-\frac{130 \frac{kJ}{mol}}{RT})$	(R3)
$CH_4 + H_2O \rightarrow CO + 3\ H_2$	$k = 7.0 \cdot 10^{6} \frac{m^3}{kmol \cdot s} [CH_4][H_2O] \exp(-\frac{126 \frac{kJ}{mol}}{RT})$	(R4)
$H_2 + 0.5\ O_2 \rightarrow H_2O$	$k = 2.2 \cdot 10^{9} \frac{m^3}{kmol \cdot s} [H_2][O_2] \exp(-\frac{109 \frac{kJ}{mol}}{RT})$	(R5)
$CO + 0.5\ O_2 \rightarrow CO_2$	$k = 1.0 \cdot 10^{10} \frac{m^3}{kmol \cdot s} [\mathrm{CO}][O_2]^{0.5} [\mathrm{H_2O}]^{0.5} \exp(-\frac{126 \frac{kJ}{mol}}{RT})$	(R6)
$CO + H_2O \leftrightarrow CO_2 + H_2$	$k_{forw} = 2.78 \cdot 10^{3} \frac{m^3}{kmol \cdot s} [\mathrm{CO}][\mathrm{H_2O}] \exp(-\frac{12.6 \frac{kJ}{mol}}{RT})$ $k_{rev} = 9.59 \cdot 10^{4} \frac{m^3}{kmol \cdot s} [\mathrm{CO_2}][\mathrm{H_2}] \exp(-\frac{46.6 \frac{kJ}{mol}}{RT})$	(R7)

Char conversion

The solid products from the devolatilization process are ash and char. In the present study, ash is assumed to be inert and char is considered as pure carbon, according to reaction (R2). As in [35], the char may undergo an oxidation, following partial oxidation, heterogeneous watergas and Boudouard reactions:

$$C + 0.5O_2 \rightarrow CO \quad \text{(R8)}$$

$$C + CO_2 \rightarrow 2CO \quad \text{(R9)}$$

$$C + H_2O \rightarrow CO + H_2 \quad \text{(R10)}$$

The reaction rate of these surface reactions is determined using the kinetic/diffusion-limited rate model, first proposed by Baum and Street [40] and has been widely used in previous numerical studies on coal combustion (see for example review by Williams et al. [41]). The rate of char conversion is influenced by both kinetics and diffusion and is determined for each of the three char conversion reactions:

$$\frac{dm_{c,i}}{dt} = -A_s \cdot p_{ox} \cdot \frac{D \cdot \omega_{c,i}}{D + \omega_{c,i}} \quad (13)$$

The kinetic rate constant of each char conversion reaction $\omega_{c,i}$ is calculated using an Arrhenius equation, the parameters of which can be found in Table 4. As for the gas phase, the heterogeneous reactions and their kinetic values correspond to those suggested in [35].

The diffusion rate constant D is described as

$$D = C_1 \cdot \frac{(\frac{T_s + T_\infty}{2})^{0.75}}{d_s} \ , \quad (14)$$

where C_1 is a model constant. The char conversion rate (equation (13)) is then incorporated into the conservation equation of both the solid phase and the gas phase as source terms.

Table 4 Reaction constants for char oxidation [35]

Reaction	Pre-exponential factor [s/m]	Activation energy [J/mol]
R8	$2.51 \cdot 10^{-3}$	$7.48 \cdot 10^{4}$
R9	$3.0 \cdot 10^{-1}$	$2.0 \cdot 10^{5}$
R10	$2.0 \cdot 10^{-3}$	$1.96 \cdot 10^{5}$

2.3 Experimental Setup

The pyrolysis and gasification experiments were previously carried out by Qin et al. at the Technical University of Denmark [34]. Beech wood sawdust (with a representative particle diameter of 310 μm) is fed into a laboratory-scale drop-tube reactor, the length and diameter of which are 2 m and 0.08 m, respectively. The reactor is electrically heated to a temperature between 1000 °C and 1400 °C. Carrier gas for the fuel is either nitrogen or air. In addition, air and/or steam are supplied into the reactor as the main gas.

Figure *2* shows the general setup of the reactor. The influence of several process parameters, among which reactor temperature, steam/carbon ratio and air ratio, on the gas production rate has been determined. More detailed information on the experimental setup can be found in the literature [34].

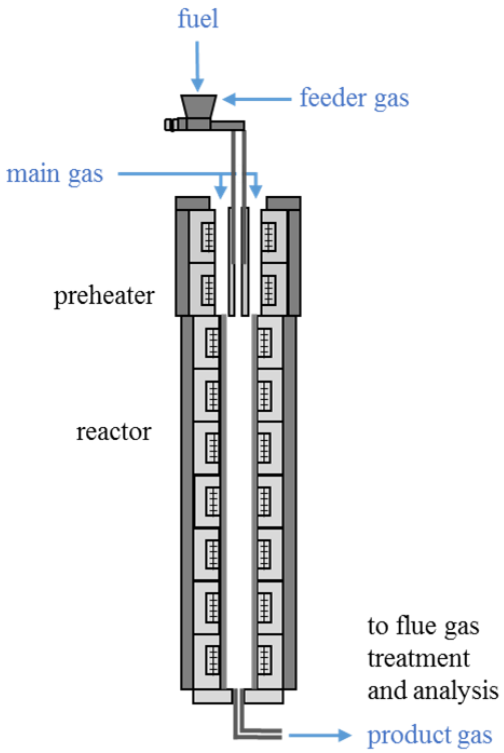

Figure 2 Reactor setup (adapted from [34]*)*

3 Results

3.1 Applicability of the model for biomass pyrolysis and gasification

Table 5 shows a list of simulated experiments using the stochastic reactor model. The labels follow the definition in [35] and [34]. In addition to the main gas flow given in Table 5, a carrier gas was used with a volumetric flow rate of 10 l/min (norm conditions) for all cases. For the pyrolysis cases P1, P2 and P3, the carrier gas was pure nitrogen. For the gasification cases G1 to G11, air (23 wt% O_2 and 77 wt% N_2) was used. Cases P1, P2 and P3 are considered pyrolysis cases also in [34], referring to the lack of air in the reactor. Accordingly, the excess air ratio is zero for these cases. However, steam is added in P2 and P3, serving as a gasification medium. The residence time of the stochastic particles in the reactor results from the geometrical dimensions and the initial conditions of the reactor. The computational time needed to achieve the results (last column in Table 5) was determined using a 3 GHz processor, 64 GB RAM, running on one core only, with 10 stochastic particles and an adaptive time stepping procedure. Note that the CFD simulations used for comparison have computational times typically of the order of several hundred CPU hours.

Table 5 List of test cases

Parameter	Case (according to [28] / [30])	T [°C]	Fuel feeding rate [g/min]	Excess air ratio λ	S/C ratio	Main gas flow rates [g/min]		Calculated residence time [s]	Computational time [min]
						Air	Steam		
Steam/Carbon ratio (molar)	P1 / wP1	1400	12.8	0	0	0	0	3.93	2.4
	P2 / wP2	1400	12.8	0	0.5	0	4.3	3.57	2.7
	P3 / wP3	1400	12.8	0	1.0	0	8.6	2.68	2.4
Reactor temperature	G1 / wT5	1000	12.8	0.3	0.5	6.9	4.3	3.99	3.4
	G2 / wT4	1100	12.8	0.3	0.5	6.9	4.3	3.68	3.2
	G3 / wT3	1200	12.8	0.3	0.5	6.9	4.3	3.42	3.9
	G4 / wT2	1300	12.8	0.3	0.5	6.9	4.3	3.18	3.1
	G5 / wT1	1400	12.8	0.3	0.5	6.9	4.3	2.97	3.7
Steam carbon ratio (molar)	G6 / wH3	1400	12.8	0.3	0	6.9	0	3.37	2.6
	G7 / wH2	1400	12.8	0.3	0.5	6.9	4.3	2.97	3.2
	G8 / wH1	1400	12.8	0.3	1.0	6.9	8.6	2.58	2.3
Excess air ratio	G9 / wL3	1400	15.3	0.25	0.5	6.9	5.2	2.64	3.7
	G10 / wL2	1400	12.8	0.3	0.5	6.9	4.3	2.97	2.5
	G11 / wL1	1400	10.9	0.35	0.5	6.9	3.7	3.09	4.4

The effect of the steam/carbon ratio on the gas production rate for wood pyrolysis and steam gasification without oxygen addition (cases P1, P2 and P3) is shown in Figure 3. In addition to the results obtained by the stochastic model, the experimental measurements [34] as well as the predictions from the CFD simulation [35] are shown.

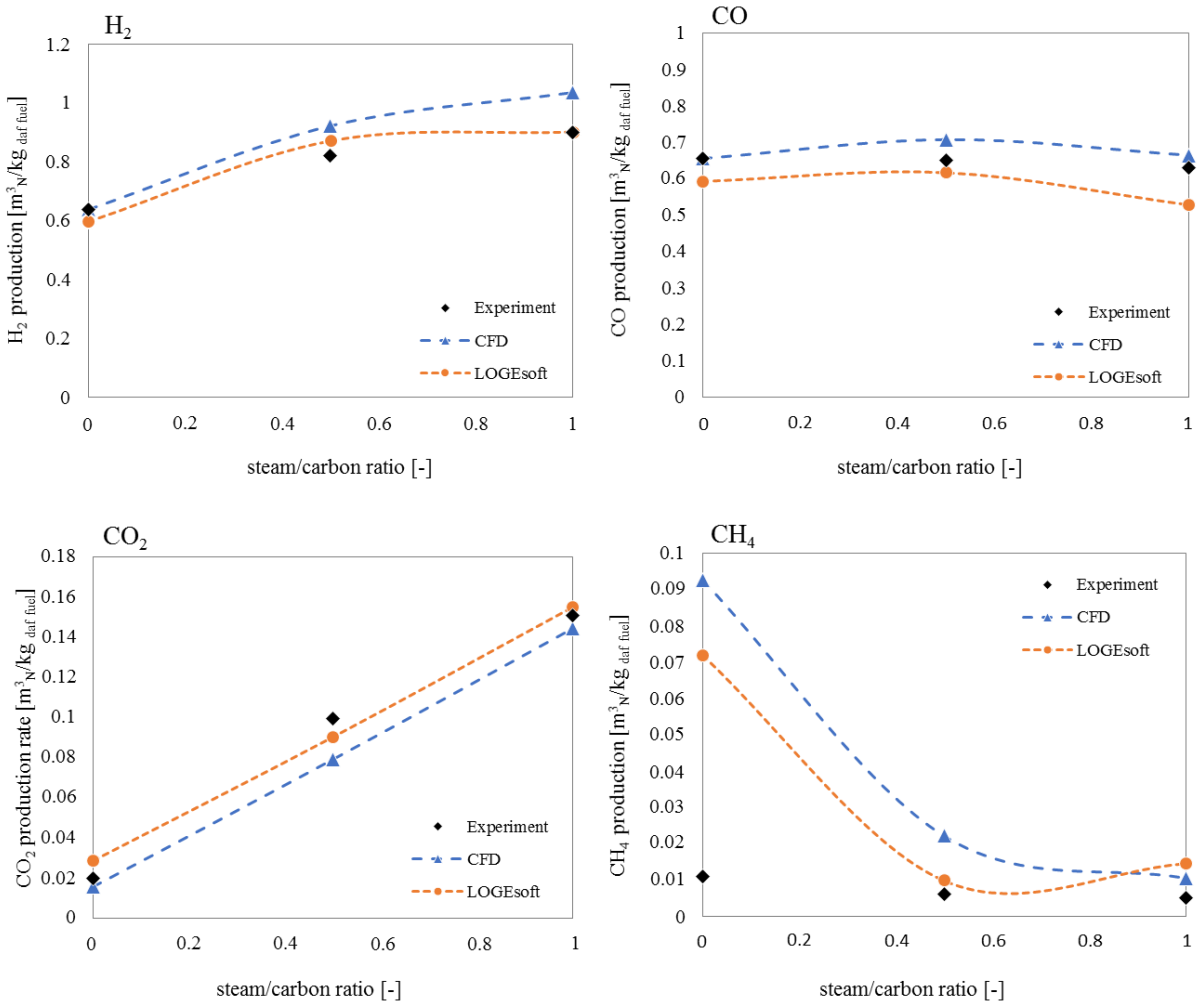

Figure 3 Effect of the steam/carbon ratio on gas production rates for wood pyrolysis (cases P1, P2 and P3 in Table 5)

It can be seen that the gas production rates of H_2 and CO_2 are quite accurately predicted by the stochastic model. The production of CO is slightly under-predicted, especially at a steam/carbon ratio of one. In the case of pure pyrolysis, the methane production rate is significantly overestimated by both the stochastic reactor model as well as the CFD simulation. However, as the total amount of methane produced is comparably little, a small error may lead to a fairly large deviation in the production rate. In addition, the very simple kinetic model assumes that only one hydrocarbon species, CH_4, is formed. Other species that are formed under real conditions are therefore summed up in the model's methane production rate, leading to the observed over-prediction.

The effect of the reactor temperature on the gas production rates in the case of gasification is shown in Figure 4. The stochastic reactor model captures the overall effect of temperature on all the product gases well. Hydrogen production

410 is over-predicted by the stochastic model for the lowest reactor temperature of 1000 °C. Its rate of increase for rising
411 temperatures is lower than for the CFD simulation and the experiment, resulting in a very good agreement at higher
412 temperatures for the stochastic model. A similar trend can be observed for CO, albeit not as significant as well as for
413 the prediction of the CO2 production rate, which as for H2 is very well predicted for higher reactor temperatures. In
414 all three cases compared to the CFD, the representation of the experimental results are equally good for both modeling
415 approaches. Methane production is however under-predicted by the stochastic model. Similar to H2, the lowest
416 reactor temperature gives the largest deviation from the experimental measurement. At the highest temperature, the
417 model performs better. As for the pyrolysis cases, the total amount of methane however is quite small leading to a
418 higher degree of error as discussed above.

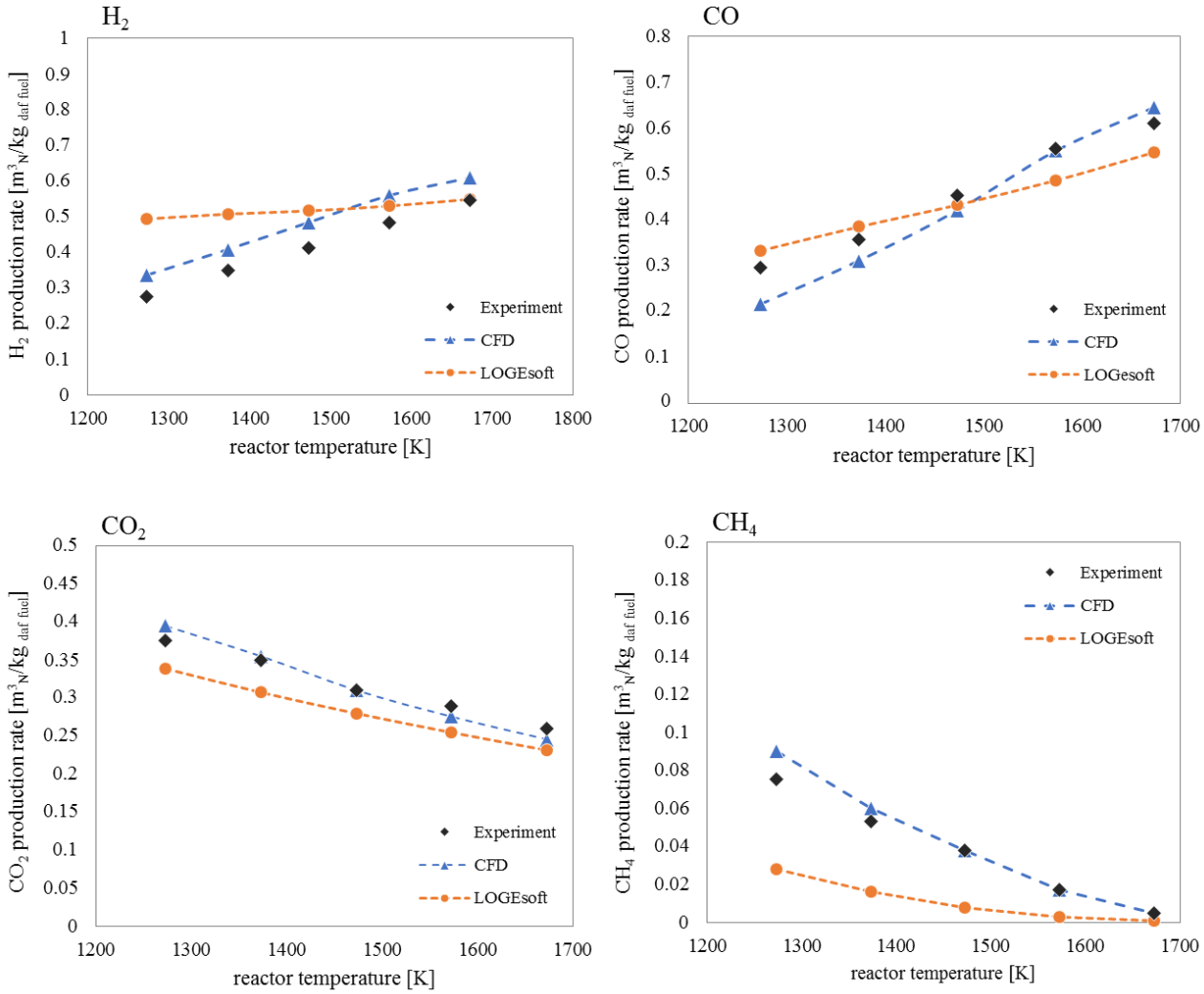

419

420 *Figure 4 Effect of the reactor temperature on gas production rates for wood gasification (cases G1 to G5)*
421
422 The influence of the molar steam/carbon ratio and the excess air ratio on the gas production rate of wood gasification
423 are shown in Figure 5. For these cases, no information on the methane production rate was available in [34]. The
424 amount of all three gases that were considered, is predicted very accurately by the stochastic reactor model. Note
425 also that experimental errors are not readily available for these data points. An uncertainty of about 10 % was

determined for comparable experiments [42]. Hence, for the results shown in Figure 5, it cannot be concluded which of the simulation approaches outperforms the other as they are equally close to the experimental results.

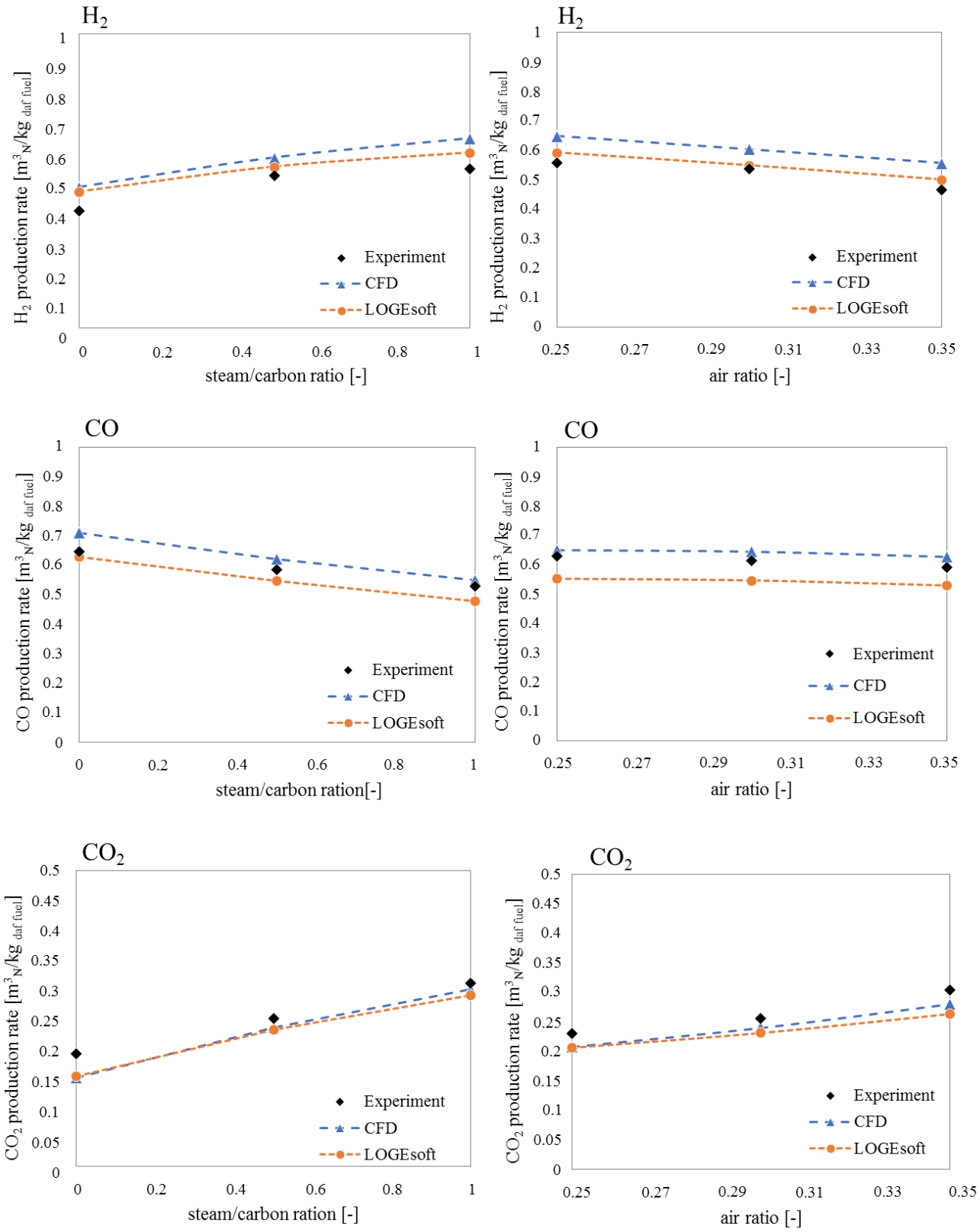

Figure 5 Left: Effect of the molar steam/carbon on gas production rates for wood gasification (cases G6 to G8); Right: Effect of the excess air ratio on gas production rates for wood gasification (cases G9 to G11)

3.2 General performance of the stochastic model

As discussed in section 2 the description of heterogeneity in the system is covered by the implemented PDF approach of the stochastic particles and turbulent mixing. The effect of the stochastic reactor on heterogeneity is studied using the settings of case G6/wT1 (Table 5). In order to decrease the influence of fast kinetics, the reactor temperature was lowered (1200 K) and the wood particle diameter increased (310×10^{-5} m). A number of 100 stochastic particles was used to emphasize the distribution of physical quantities throughout the simulations. The case was modeled with a given model constant defining the wall heat transfer (C_h=40). Figure 6 (top) shows the gas temperature distribution over all 100 stochastic particles for this case at a reactor length of 0.15 m. For this given case the fluctuations of gas temperature in the reactor range over approximately 15 K scattered around a mean value with a significant number of outliers (similar results are found for solid and pore gas temperatures, not shown here). This behavior in the temperature will have a direct effect on the species distribution over the particles. Figure 6 (bottom) shows the mass fraction of CO in all particles for the same stochastic constant. The mass fractions of other species behave in the same manner. This clearly reveals that the stochastic reactor approach very efficiently captures the variations in composition that develops in such reactors due to mixing, affecting the predictability of the final product yield distribution. It will be important to establish the sensitivity of certain model constants on the final results and this will be the subject for future studies.

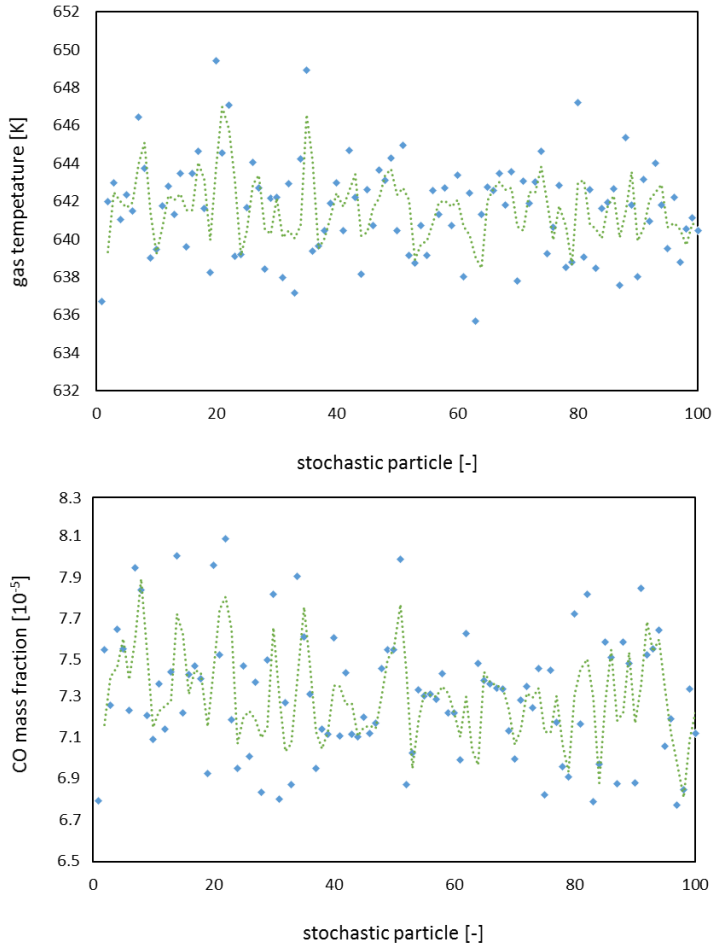

Figure 6 Gas temperature (top) and CO mass fraction (bottom) at a reactor length of 0.15 m (dashed lines indicate the moving average with a period of 2)

4 Conclusion

A stochastic reactor model for a PaSPFR has been used to model an experimental series on biomass pyrolysis and gasification, performed in a drop tube reactor at high temperatures (1000-1400 °C). The influence of reactor temperature, steam/carbon-ratio and air ratio on the production rate of the gas components H_2, CO, CO_2 and CH_4 has been determined. The performance of the stochastic model is directly compared to CFD model predictions employing the same kinetic model on the same experimental setup with very good agreement for most conditions. For low reactor temperatures, the prediction of hydrogen and methane shows a significant deviation from the experimental results of wood gasification. These cases are matter of future investigations. Methane is also under-predicted for one of the pyrolysis cases for both CFD and SRM calculations. In most cases however, the product gas composition is predicted with good accuracy by the stochastic approach, comparable to the CFD simulation, suggesting that the observed deviations can be attributed to the rather simple chemical model employed in both modelling approaches, especially for the gas phase reactions, rather than the simplified reactor model.

The strength of the stochastic reactor approach is the description of main properties and processes by a probability density function instead of continuously resolving transport equations in all spatial dimensions. This makes the approach computationally efficient by decreasing the computational time from several hundred CPU hours to less than 5 minutes compared to CFD. This is appealing for situations where large systems are under investigation or when many different conditions are to be studied. It is shown that by defining the stochastic properties of the model appropriately, a sophisticated description of the physical properties is possible. The model can be coupled with a more detailed chemical mechanism, as will be the subject of future work. Future work also includes the implementation of a more comprehensive treatment of the physical particle size evolution, which is important in many applications. It therefore also offers a suitable and efficient tool for the development and validation of kinetic models for biomass conversion processes, before such models are applied in CFD.

Acknowledgement

The authors are thankful for the financial support from the Research Council of Norway, from the industry partners of the BioCarb+ project (Elkem AS, Norsk Biobrensel AS, AT Biovarme AS, Eyde-nettverket, Saint Gobain Ceramic Materials AS, Eramet Norway AS, Alcoa Norway ANS) and from the SMARTCAT COST network.

Nomenclature

A	surface area	[m^2]
A	frequency factor, pre-exponential factor	[unit dependent on reaction]
c	species concentration	[mol/m^3]
C_1	mass diffusion rate constant	[$s/K^{0,75}$]
C_h	model constant	[-]
C_p	heat capacity	[J/(kgK)]
C_ϕ	mixing constant	[-]
d	particle diameter	[m]
D	diffusion rate constant	[s/m]
E	activation energy	[kJ/mol]
F_ϕ	mass density function	[-]
h	specific enthalpy	[J/kg]
H	specific heat	[J/kg]
h_n	heat transfer fluctuation	[K]
k	reaction rate (mole-based)	[$kmol/(m^3s)$]
k_m	mass transfer coefficient	[m/s]
m	mass	[kg]
n	number, numbered item (non-specific)	[-]
p	pressure	[N/m^2]

$\mathbf{Q_i}$	source term function	[-]
q_{rad}	radiation term	[J/(m^{2}s)]
t	time	[s]
T	temperature	[K]
V	volume	[m^3]
W	molecular mass	[kg/mol]
Y	species mass fraction	[-]
α	heat transfer coefficient	[W/(m^{2}K)]
β	porosity source factor	[-]
β_m	mixing constant	[-]
ε	porosity	[-]
ε	emissivity	[-]
ρ	density	[kg/m^3]
σ	Stefan Boltzmann constant	[W/(m^{2}K^4)]
τ	time step size	[s]
τ_{mix}	mixing time	[s]
$\boldsymbol{\phi}$	random variable	[unit depending on the variable]
$\boldsymbol{\psi}$	realization of any random variable	[unit depending on the variable]
ω	reaction rate, chemical source term	[kg/(m^{2}s)] or [kg/(m^{3}s)], depending on the subscript

Subscripts

s	solid phase
g	bulk gas phase
p	pore gas phase
i, j	Species i, j
m	mass
w	wall
rad	radiant, due to radiation
pyr	pyrolysis
c, char	char
par	particle
∞	surrounding
total	total, referring to an entity

Literature

[1] A. J. Ragauskas *et al.*, "The path forward for biofuels and biomaterials.," *Science*, vol. 311, no. 5760, pp. 484–9, 2006.

[2] W. Gorton and J. Knight, "Oil from biomass by entrained-flow pyrolysis," *Biotechnol. Bioeng. Symp.*, vol. 14, pp. 15–20, 1984.

[3] R. Font, A. Marcilla, E. Verdii, and J. Devesa, "Kinetics of the Pyrolysis of Almond Shells and Almond Shells Impregnated with CoC12 in a Fluidized Bed Reactor and in a Pyroprobe 100," *Ind. Eng. Chem. Res.*, no. 3, pp. 1846–1855, 1990.

[4] B. M. Wagenaar, W. Prins, and W. P. M. van Swaaij, "Pyrolysis of biomass in the rotating cone reactor: modelling and experimental justification," *Chem. Eng. Sci.*, vol. 49, no. 24, pp. 5109–5126, 1994.

[5] C. Di Blasi and C. Branca, "Kinetics of Primary Product Formation from Wood Pyrolysis," *Ind. Eng. Chem. Res.*, vol. 40, no. 23, pp. 5547–5556, 2001.

[6] C. Branca, A. Albano, and C. Di Blasi, "Critical evaluation of global mechanisms of wood devolatilization," *Thermochim. Acta*, vol. 429, no. 2, pp. 133–141, 2005.

[7] C. DiBlasi, "Modeling chemical and physical processes of wood and biomass pyrolysis," *Prog. Energy Combust. Sci.*, vol. 34, no. 1, pp. 47–90, 2008.

[8] P. Quicker and K. Weber, *Biokohle. Herstellung, Eigenschaften und Verwendung von*

Biomassekarbonisaten. Wiesbaden: Springer Vieweg, 2016.
[9] P. A. Brownsort, "Biomass Pyrolysis Processes: Review of Scope, Control and Variability," *Biomass*, p. 38, 2009.
[10] J. Lédé, "Biomass Fast Pyrolysis Reactors: A Review of a Few Scientific Challenges and of Related Recommended Research Topics," *Oil Gas Sci. Technol. – Rev. d'IFP Energies Nouv.*, vol. 68, no. 5, pp. 801–814, Sep. 2013.
[11] C. H. Bamford, J. Crank, and D. H. Malan, "Mathematical Proceedings of the Cambridge Cambridge Philosophical Society : The combustion of wood . Part I," no. 1946, pp. 166–182, 1945.
[12] D. Lathouwers and J. Bellan, "Modeling of dense gas–solid reactive mixtures applied to biomass pyrolysis in a fluidized bed," *Int. J. Multiph. Flow*, vol. 27, no. 12, pp. 2155–2187, Dec. 2001.
[13] M. Oevermann, S. Gerber, and F. Behrendt, "Euler–Lagrange/DEM simulation of wood gasification in a bubbling fluidized bed reactor," *Particuology*, vol. 7, no. 4, pp. 307–316, Aug. 2009.
[14] S. Gerber, F. Behrendt, and M. Oevermann, "An Eulerian modeling approach of wood gasification in a bubbling fluidized bed reactor using char as bed material," *Fuel*, vol. 89, no. 10, pp. 2903–2917, Oct. 2010.
[15] J. Bruchmüller, B. G. M. van Wachem, S. Gu, K. H. Luo, and R. C. Brown, "Modeling the thermochemical degradation of biomass inside a fast pyrolysis fluidized bed reactor," *AIChE J.*, vol. 58, no. 10, pp. 3030–3042, Oct. 2012.
[16] E. Ranzi, M. Corbetta, F. Manenti, and S. Pierucci, "Kinetic modeling of the thermal degradation and combustion of biomass," *Chem. Eng. Sci.*, vol. 110, pp. 2–12, 2014.
[17] E. Ranzi, S. Pierucci, P. C. Aliprandi, and S. Stringa, "Comprehensive and detailed kinetic model of a traveling grate combustor of biomass," *Energy and Fuels*, vol. 25, no. 9, pp. 4195–4205, 2011.
[18] N. Prakash and T. Karunanithi, "Kinetic Modeling in Biomass Pyrolysis – A Review," *J. Appl. Sci. Res.*, vol. 4, no. 12, pp. 1627–1636, 2008.
[19] N. Prakash and T. Karunanithi, "Advances in modeling and simulation of biomass pyrolysis," *Asian Journal of Scientific Research*, vol. 2, no. 1. pp. 1–27, 2009.
[20] M. Puig-Arnavat, J. C. Bruno, and A. Coronas, "Review and analysis of biomass gasification models," *Renew. Sustain. Energy Rev.*, vol. 14, no. 9, pp. 2841–2851, 2010.
[21] Ø. Skreiberg, P. Kilpinen, and P. Glarborg, "Ammonia chemistry below 1400 K under fuel-rich conditions in a flow reactor," *Combust. Flame*, vol. 136, no. 4, pp. 501–518, Mar. 2004.
[22] E. Houshfar, Ø. Skreiberg, P. Glarborg, and T. Løvås, "Reduced chemical kinetic mechanisms for NOx emission prediction in biomass combustion," *Int. J. Chem. Kinet.*, vol. 44, no. 4, pp. 219–231, Apr. 2012.
[23] D. H. Lee, H. Yang, R. Yan, and D. T. Liang, "Prediction of gaseous products from biomass pyrolysis through combined kinetic and thermodynamic simulations," *Fuel*, vol. 86, no. 3, pp. 410–417, Feb. 2007.
[24] S. Septien, S. Valin, M. Peyrot, B. Spindler, and S. Salvador, "Influence of steam on gasification of millimetric wood particles in a drop tube reactor: Experiments and modelling," *Fuel*, vol. 103, pp. 1080–1089, Jan. 2013.
[25] Aspentech, "Aspen Plus," 2016. [Online]. Available: http://www.aspentech.com/products/solids-aspen-plus/. [Accessed: 14-Dec-2016].
[26] D. T. Pratt, "Mixing and chemical reaction in continuous combustion," *Prog. Energy Combust. Sci.*, vol. 1, no. 2–3, pp. 73–86, 1976.
[27] L. A. Spielman and O. Levenspiel, "A Monte Carlo Treatment for Reacting and Coalescing Dispersed Phase Systems," *Chem. Eng. Sci.*, vol. 20, no. 3, pp. 247–254, 1965.
[28] A. R. Masri, P. A. M. Kalt, Y. M. Al-Abdeli, and R. S. Barlow, "Turbulence – chemistry interactions in non - premixed swirling flames," *Combust. Theory Model.*, vol. 11, no. 5, pp. 653–673, 2007.
[29] J. Y. Chen, "Stochastic Modeling of Partially Stirred Reactors," *Combust. Sci. Technol.*, vol. 122, no. 1, pp. 63–94, 1997.
[30] S. M. Correa, "Turbulence-Chemistry Interaction in the Intermediate Regime of premixed Combustion," *Combust. Flame*, vol. 60, p. Vol. 93, pp: 41-60, 1993.

[31] M. Balthasar, F. Mauss, A. Knobel, and M. Kraft, “Detailed modeling of soot formation in a partially stirred plug flow reactor,” *Combust. Flame*, vol. 128, no. 4, pp. 395–409, 2002.
[32] A. Bhave and M. Kraft, “Cambridge Centre for Computational Chemical University of Cambridge Partially Stirred Reactor Model : Analytical Solutions and Numerical Convergence Study of PDF / Monte Carlo Method,” *Chem. Eng.*, no. 7, 2002.
[33] S. Mosbach *et al.*, “Dual injection homogeneous charge compression ignition engine simulation using a stochastic reactor model,” *Int. J. Engine Res.*, vol. 8, no. 1, pp. 41–50, Jan. 2007.
[34] K. Qin, P. A. Jensen, W. Lin, and A. D. Jensen, “Biomass Gasi-fi-cation Behavior in an Entrained Flow Reactor : Gas Product Distribution and Soot Formation,” *Energy & Fuels*, 2012.
[35] X. K. Ku, T. Li, and T. Lovas, “Eulerian-Lagrangian Simulation of Biomass Gasification Behavior in a High-Temperature Entrained-Flow Reactor,” *Energy & Fuels*, vol. 28, no. 8, pp. 5184–5196, 2014.
[36] LOGE AB, LOGEsoft v1.4 software manuals, 2016, http://www.loge.se
[37] A. Bhave, M. Balthasar, M. Kraft, and F. Mauss, “Analysis of a natural gas fuelled homogeneous charge compression ignition engine with exhaust gas recirculation using a stochastic reactor model,” *Int. J. Engine Res.*, vol. 5, no. 1, pp. 93–104, Jan. 2004.
[38] R. L. Curl, “Dispersed phase mixing: I. Theory and effects in simple reactors,” *AIChE J.*, vol. 9, no. 2, pp. 175–181, 1963.
[39] W.-C. R. Chan, M. Kelbon, and B. B. Krieger, “Modelling and experimental verification of physical and chemical processes during pyrolysis of a large biomass particle,” *Fuel*, vol. 64, no. 11, pp. 1505–1513, Nov. 1988.
[40] M. M. Baum and P. J. Street, “Predicting the Combustion Behaviour of Coal Particles,” *Combust. Sci. Technol.*, vol. 3, no. 5, pp. 231–243, 1971.
[41] A. Williams, R. Backreedy, R. Habib, J. M. Jones, and M. Pourkashanian, “Modelling coal combustion: The current position,” *Fuel*, vol. 81, no. 5, pp. 605–618, 2002.
[42] C. Dupont, J. M. Commandré, P. Gauthier, G. Boissonnet, S. Salvador, and D. Schweich, “Biomass pyrolysis experiments in an analytical entrained flow reactor between 1073 K and 1273 K,” *Fuel*, vol. 87, no. 7, pp. 1155–1164, 2008.